LINEAR STABILITY ANALYSIS OF TIME-DEPENDENT IMMISCIBLE FLOW DISPLACEMENTS IN POROUS MEDIA

Lins, T. F. and Azaiez J.*
*Author for correspondence
Department of Chemical and Petroleum Engineering,
The University of Calgary,
Calgary, Alberta,
Canada,
E-mail: azaiez@ucalgary.ca

ABSTRACT

Flow displacements in porous media are encountered in a wide variety of fields, in particular in the energy and environmental sectors. Such flows are prone to a hydrodynamic instability that develops as a result of differences in the physical properties of the different fluids, namely their viscosity and/or density. A simple and inexpensive way to attenuate the instabilities is to implement time-dependent injection schemes.

In this study, flows in radial two- dimensional homogeneous porous media are modelled. A low-viscosity fluid is injected radially at the centre of the cell to displace a more viscous one. The model equations are developed and a linear stability analysis is carried out. Different time-dependent velocity profiles are considered and the effects of different flow parameters are analysed and compared with the corresponding constant injection velocity flows. For consistency, the comparisons are conducted on the basis that all injection schemes including the constant one, result in the same total amount of injected fluid. Qualitative analyses are conducted using different measures of the growth of the instability and are used to determine the changes induced by the time-dependent injections. These changes in the flow dynamics can be used to control the degree of mixing between the two fluids and to optimize a variety of flow displacements in porous media.

INTRODUCTION

Hydrodynamic instabilities can develop at the interface between two fluids flowing in a porous medium. These instabilities manifest themselves in the form of finger-like structures at the interface between the two fluids. In the case of homogeneous porous media, the instability develops as a result of viscosities mismatch and is referred to as viscous fingering and/or densities mismatch where it is known as the Rayleigh-Taylor instability. Both instabilities are encountered in a variety of processes that span a wide range of fields that include chemical, petroleum and environmental sectors. Hence a better understanding of these instabilities is crucial for the design, optimization and improvement of numerous processes encountered in the operation of packed bed reactors, production and enhanced recovery of oil, decontamination of soil as well as the sequestration of carbon dioxide

Extensive studies have been conducted to analyze the effects of different factors on the instability including the viscosity ratio [1], dispersion [2], non-Newtonian rheological behavior of the fluids [3], chemical reaction [1], heat transfer [4] and flow configuration [5] among others. Detailed literature reviews that date back to the 1980s and 1990s are found in [6] and [7].

The vast majority of existing studies have focused on miscible displacements when dispersion plays an important role in addition to the viscosity/density ratios and the injection rates. However in numerous practical applications, the flow displacements are immiscible and surface tension forces become a major factor in the development and subsequent fate of the instability.

Immiscible flows were studied experimentally. Paterson [8] investigated the width of fingers and developed equations to fit the radius of the tip and base of fingers based on the injection flow rate, time and arbitrary parameters. In a later study, Chen [9] analyzed the effect of plate roughness and flow rate as well as interfacial tension. It was observed that for smooth plates, fingering patterns are strongly influenced by the flow rate, with narrower fingers occurring as the flow rate increases. In rough plates, fingers tend to branch more easily. Low flow rates for both smooth and rough plates enable the fingers to be more compact. The same author later observed the development of fingers at later long times after multiple splitting, suggesting that immiscible patterns can be similar at the same dimensionless time [10]. In a subsequent study, Praud and Swinney [11] found an asymptotic behavior for the ratio of the fingers' radius over the gap thickness in a radial Hele-Shaw cell.

Many miscible displacement experiments have also been performed under a variety of conditions. Chen demonstrated that fractal dimensions remain constant [5]. Much of the experimental work on miscible flow has however been conducted for rectilinear geometries.

The stability of immiscible displacement in a radial geometry has been studied by Wilson [12] and later by Paterson [8]. An equation relating the growth rate of the instabilities with the radius of the interface, the surface tension, the mobility ratio as well as the injection rate was derived. Later variations on this equation describing the growth rate of instabilities were developed. In particular Park and Homsy [13] derived an equation for the pressure jump at the interface. Their study was based on a three dimensional analysis, where the displaced fluid leaves a thin layer in the Hele-Shaw cell. Experiments validated the relationship developed to predict the number of fingers more accurately. Subsequently Martyushev and Birzina [14] used this pressure jump expression to develop a new equation for the growth rate of instabilities in the front for radial instabilities flows in the case of constant injection rate and constant pressure.

Miranda and Widom [15] investigated the effects of non-linear terms in the growth rate of instabilities. Based on their results from the linear portion of the growth rate, it was found that the number of fingers is dictated by the mode at which its amplitude is the largest. A large number of fingers (n) often leads to finger splitting, thus requiring the application of non-linear analysis.

Most of the existing studies dealing with time-dependent injection schemes have been based on Linear Stability Analysis (LSA.) Dias et al. attempted to minimize the integral of growth rate over time [16]. With the aid of some reasonable approximations, it was found that a linear injection rate would provide more stable growth of the interface. In a subsequent study [17], it was observed that for a 3-dimensional, spherical system, the best injection scheme is related to the square of time. It is important to note that in both scenarios, the proposed flow rate scheme is not dependent on the properties of the fluid or the medium. These results were recently tested by Huang and Chen [18] for immiscible, partially miscible and miscible radial flows in a Hele-Shaw Cell. It was demonstrated that for immiscible and partially miscible flows, the linear injection scheme can substantially reduce the fingering instabilities, reducing the interfacial length when compared to the constant injection scheme. Miscible flows, on the other hand, showed opposite trends.

The application of cyclic time-dependent injection schemes to control fingering was investigated mostly for miscible displacement [19]. More complex scenarios have also been observed. Daripa [20] investigated multi-layered flow instability and proposed systems where stable flow would occur for three to multiple layers of fluid.

It was observed that the equation presented by Paterson et al. [8] tends to overestimate the growth rate of disturbances compared to more complex models, so that its use as a tool to identify injection schemes that reduce instability is safe.

NOMENCLATURE

M	[]	Mobility ratio
p	[Pa]	Pressure
R	[m]	Radius
R_0	[m]	Core radius of injection
t	[s]	time
T	[s]	Period
U	[m/s]	*velocity*
U_n	[m/s]	Normal velocity

Special characters

β	[m^3s/kg]	Mobility
Γ	[]	amplitude
ζ	[m]	Amplitude of instability in the linear regime
θ	[]	angle
κ	[1/m]	Curvature
λ	[1/s]	Growth rate
μ	[Pa.s]	viscosity
σ	[]	Relative growth rate
τ	[m^2]	Surface tension
ϕ	[1/s]	Injection strength
φ	[]	Phase shift

Subscripts

1	Fluid 1: less viscous
2	Fluid 2: more viscous
n	Mode (1,2,3…)
c	constant
e	exponential
l	linear
s	sinusoidal
TD	Time-dependent

MODEL AND MATHEMATICAL FORMULATION

The considered model consists of a two-dimensional homogeneous porous medium with constant permeability K, where the flow develops radially from a centre source. A fluid of viscosity μ_1 is injected in the centre of the domain and displaces radially a second fluid of viscosity μ_2, that initially occupies the medium. The two fluids are assumed to be fully immiscible with a surface tension τ. The displacement is isothermal, non-reactive and the fluids are assumed to be Newtonian. A schematic of the flow is shown in Figure 1.

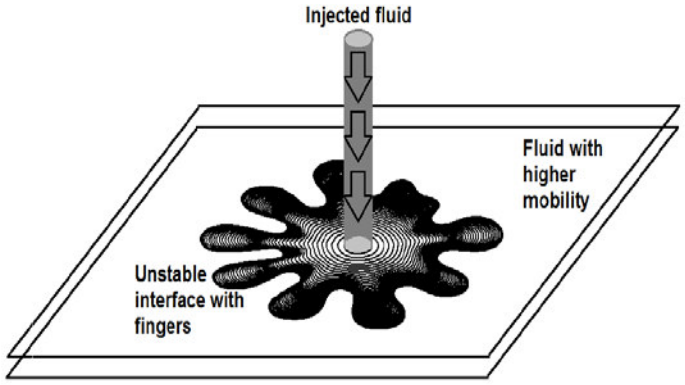

Figure 1 Schematic of the flow displacement

The mathematical model describing the immiscible displacement consist of the continuity equation (mass conservation) and Darcy's law:

$$\nabla.\mathrm{U} = \begin{cases} \phi, & r \le R_0 \\ 0, & r > R_0 \end{cases} \quad (1)$$

$$\mathrm{U} = \begin{cases} -\beta_1 \nabla p, & r \le R(\theta,t) \\ -\beta_2 \nabla p, & r > R(\theta,t) \end{cases} \quad (2)$$

In the above model, the equations are formulated in each region occupied by either fluid1 or fluid2. The continuity equation involves a source injection rate ϕ in a specific region of the domain, determined by a radius R_0, which also corresponds to the initial radius of the interface. Darcy's law expresses the proportionality between the fluid velocity (U) and the pressure gradient through the mobility ($\beta_i = {}^{K}/_{\mu_i}, i = 1,2$) corresponding to the ratio of the medium's permeability (K) and the fluid viscosity (μ). The interface between the two fluids at any time (t) and angle (θ) is $R(\theta,t)$. Kinematic and dynamic jump conditions at the interface in the form of continuity of the normal velocity ($\mathrm{U_n}$) and Laplace-Young equations are used:

$$[\mathrm{U}_n]_1^2 = 0 \quad (3)$$

$$[p]_1^2 = \tau\kappa \quad (4)$$

Where the brackets refer to the difference of values at the interface between the injected fluid (fluid1) and the one already present in medium (fluid2). In the above equations, κ is the curvature of the interface while τ is the surface tension.

The objective of this study is to analyse the development of the instability under time-dependent injection flows. In what follows the exact forms of the three considered time-dependent injection rates as well as the constant one, are presented.

-Constant injection: $Q_c = Q_0$, (5)

-Sinusoidal injection: $Q_s(\mathrm{t}) = Q_0\left[1 + \Gamma \sin\left(\frac{2\pi \mathrm{t}}{\mathrm{T}}\right)\right]$ (6)

-Exponential injection: $Q_e(\mathrm{t}) = Cexp(Dt)$ (7)

-Linear injection: $Q_l(t) = mt + b$ (8)

In the above equation, Q_0 is the constant injection flow rate corresponding to an injection strength; $\phi_0 = Q_0/\pi R_0^2$. The cyclic injection scheme is characterized by its relative amplitude Γ and period; T. Note that when $\Gamma \leq 1$, the displacement rate will be positive $(Q(\mathrm{t}) \geq 0)$ and the flow will undergo simple injection while for $\Gamma > 1$ it will alternate between injection $(Q(\mathrm{t}) > 0)$ and extraction $(Q(\mathrm{t}) < 0)$. The exponential injection scheme, and the linear injection scheme are dependent on the constant C and D, and m and b, respectively which shall be defined later. It is important to note here that all three time-dependent schemes will result in the same amount of injected fluid over a period. This implies that the net injected flow in both the time-dependent and constant velocity displacements is the same.

The model equations are formulated in dimensionless form using the following scales: $1/\phi_0$ for time, R_0 for length, $\phi_0 R_0$ for velocity, $R_0^3\phi_0/\beta_2$ for surface tension and $\phi_0 R_0^2/\beta_2$ for pressure. The resulting dimensionless forms are: (* indicates dimensionless quantities):

$$\nabla^*.\mathrm{U}^* = \begin{cases} \phi^*, & r^* \leq 1 \\ 0, & r^* > 1 \end{cases} \quad (9)$$

$$\mathrm{U}^* = \begin{cases} -\mathrm{M}\nabla^* p^*, & r^* \leq R^*(\theta, \mathrm{t}^*) \\ -\nabla p^*, & r^* > R^*(\theta, \mathrm{t}^*) \end{cases} \quad (10)$$

$$[p^*]_1^2 = \tau^*\kappa^*, [\mathrm{U}_n^*]_1^2 = 0 \quad (11)$$

$$Q_c{}^* = 1, Q_s{}^*(\mathrm{t}^*) = \left[1 + \Gamma \sin\left(\frac{2\pi \mathrm{t}^*}{\mathrm{T}^*}\right)\right], Q_e{}^*(\mathrm{t}^*) = Cexp(Dt^*), Q_L^*(t^*) = mt^* + b \quad (12)$$

The notation used in the above expressions are:

$\mathrm{U}^* = \mathrm{U}/R_0\phi_0$, $\mathrm{U}_n^* = \mathrm{U}_n/R_0\phi_0$, $\mathrm{t}^* = \mathrm{t}\phi_0$, $r^* = r/R_0$, $R^* = R/R_0$, $\phi^* = \phi/\phi_0$, $\mathrm{T}^* = \mathrm{T}\phi_0$,

$\tau^* = \tau\beta_2/R_0^3\phi_0$, $\kappa^* = \frac{\kappa}{R_0}$, $p^* = p\phi_0 R_0^2/\beta_2$,

$Q^*(\mathrm{t}) = Q(\mathrm{t})/Q_0 = Q(\mathrm{t})/\pi R_0^2\phi_0$

and $\mathrm{M} = \beta_1/\beta_2$ is the mobility ratio.

The dimensionless parameters that govern the displacement and that will be analysed in this study are M and τ^*.

Henceforth, all the asterisks are dropped as all quantities are presented in dimensionless form.

LINEAR STABILITY FORMULATION

The relationship between the growth rate and the other parameters that govern the displacement in a radial geometry are the following. [16]

$$\frac{1}{\zeta_n(t)}\frac{d\zeta_n(t)}{dt} = \sigma_n dt \quad (13)$$

$$\zeta_n(t) = \exp\left(\int_0^{t_c} \sigma_n(t)dt\right) \quad (14)$$

$$\sigma_n(t) = \frac{Q}{2\pi R^2}(An - 1) - \frac{\alpha}{R^3}n(n^2 - 1) \quad (15)$$

In the above expressions, n is the mode, $\sigma_n(t)$ is the growth rate, $A = (M-1)/(M+1)$, $\alpha = \tau M/(M+1)$.

A large growth rate ensures that the amplitude of the waves in linear regime is large.

FUNCTIONS FOR STABILITY ANALYSIS

The minimization of $\zeta_n(\mathrm{t})$ has been previously used to find injection schemes that attenuate instabilities [16]. The exponential of the integral of the growth rate over time is obtained using simple numerical integration techniques, such as the trapezoidal rule. A large value of $\zeta_n(\mathrm{t})$ would likely indicate an increase in the amplitude and the rate at which fingers grow in the linear regime. The value of n is chosen as n_{max}, which is the mode that results in the maximum growth rate of instabilities. The mode n_{max} can be found by determining the mode where $d\sigma/dn=0$

To quantify the differences between the time-dependent and constant schemes, a function $\mathrm{G(t)}$ which is a measure of the integral of the growth rate difference, is adopted:

$$G(t) = \ln(\zeta_n(t)_{TD}) - \ln(\zeta_n(t)_c) \quad (16)$$

where $\ln(\zeta_n(t)_{TD})$ and $\ln(\zeta_n(t)_c)$ are the integrals of the growth rate $\sigma_n(t)$ over time for a specific time-dependent (TD) injection rate, and for the constant injection case respectively. A positive $\mathrm{G(t)}$ indicates that the flow is more unstable than the case with the constant injection.

To ensure that the different injection schemes can be consistently compared, all flow schemes are such that they lead to the same cumulative Q. Furthermore, all results are presented for M=10 and $\tau = 1 \times 10^{-3}$, unless stated otherwise. The reported results for the growth rate of instabilities ($\lambda_\mathrm{n}(\mathrm{t})$) are all made relative to the value of $\sigma_n(t)$ for a constant injection scheme, so that:

$$\lambda_n(\mathrm{t}) = (\sigma_\mathrm{n}(\mathrm{t})_{\mathrm{TD}} - \sigma_\mathrm{n}(\mathrm{t})_\mathrm{c})/\sigma_n(\mathrm{t})_c. \quad (17)$$

In all the subsequent results, it is important to notice the difference between $\lambda_n(\mathrm{t})$ and $G(t)$. While $\lambda_\mathrm{n}(\mathrm{t})$ only indicates the propensity of a system to experience instability at any given time and injection rate, the function $G(t)$ expresses the *cumulative* effect of instabilities from the start of the injection process up to a given point in time. As a matter of reference, the profiles for $\mathrm{Q(t)}$, $\ln(\zeta_n(t)_c)$, and $\lambda_\mathrm{n}(\mathrm{t})$ for the constant injection scheme are shown in Figure 2.

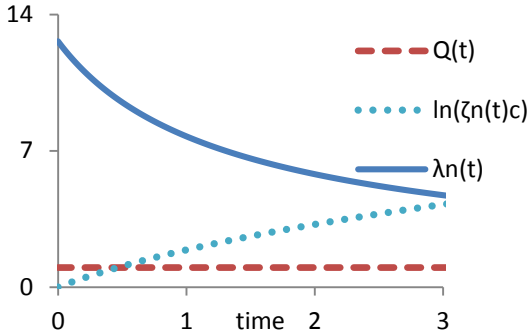

Figure 2 Profiles of injection rate Q(t), the logarithm of the amplitude of instability $\ln(\zeta_n(t)_c)$, and the growth rate $\lambda_n(t)$ for the constant injection scheme

TRENDS AND RESULTS

The results will be first discussed for the cyclic sinusoidal scheme, where in particular the effects of the period, amplitude and shift are examined. This is followed by a discussion of results for the monotonic injection schemes.

Cyclic Injection Schemes

In what follows, the effects of the period (T) are evaluated. Figure 2 and Figure 3 depict the variations with time of the injection rate; Q(t), the growth rate; $\lambda_n(t)$ and the quantifying function; $G(t)$, for two values of the period and fixed amplitude and phase shift. Based on these figures, the growth rate is essentially in phase with the injection rate. This is in accordance with the growth rate equation. The function $G(t)$ tends however to be out of phase with the other variables, likely because it is dependent on the integral of the growth rate over time. This implies that its derivative is in phase with the growth rate. More importantly, it is found that the larger period results in smaller values of the quantifying function $G(t)$ which implies a stronger attenuation of the flow instability. Note however that the values of $G(t)$ at $t = t_c$ (the end of the injection process) are virtually the same for both periods.

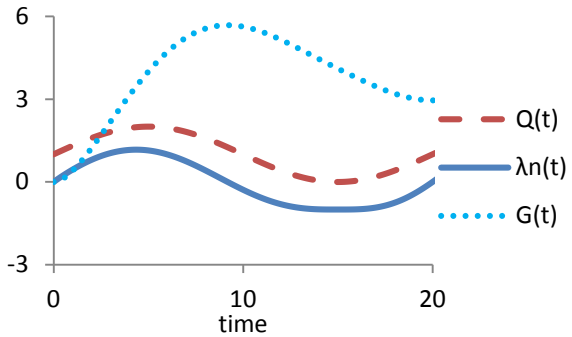

Figure 3 Profile of injection rate (Q), normalized growth rate ($\lambda_n(t)$) and integral of growth rate over time ($\boldsymbol{G(t)}$), at T=20, Γ=1, φ=0

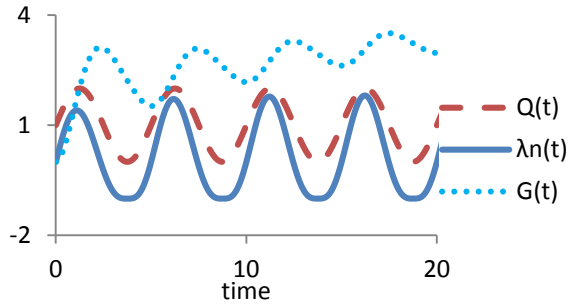

Figure 4 Profile of injection rate Q(t), normalized growth rate ($\lambda_n(t)$) and integral of growth rate over time (G(t)), at T=5, Γ=1, φ=0

The effect of varying the amplitude of the injection (Γ) was also investigated at a fixed period (T=5). Figures 4, 5 and 6 show the results for Γ =1, 0.5 and 4, respectively. For the two scenarios with amplitudes smaller than one and hence displacements involving only injections, an increase in the amplitude tends to enhance the flow instability as exemplified by the larger values of $G(t)$. This increase in the instability is however much larger for amplitudes ($\Gamma > 1$) where injection alternates with extraction, leading to values of $G(t)$ one order of magnitude larger than those for $\Gamma \leq 1$ (see Figure 5). It is interesting to notice that the growth rate $\lambda_n(t)$ is limited in how negative it can become, and this is more visible as the amplitude increases. It can also be seen that during these intervals, the function $G(t)$ diminishes slightly, but never enough so as to become negative. This implies that once the interface becomes disturbed and instabilities have developed, it is not possible to revert back to a stable interface even if extraction is employed.

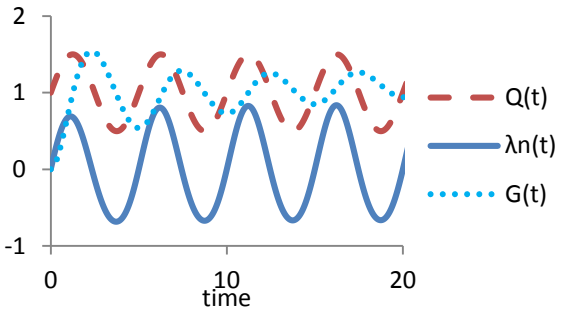

Figure 5 Profile of injection rate (Q), normalized growth rate ($\lambda_n(t)$) and integral of growth rate over time ($\boldsymbol{G(t)}$), at T=5, Γ=0.5, φ=0

The role of the phase shift can substantially influence the occurrence and extent of instabilities. Variations of $G(t)$ with time and with the phase shift φ are presented in Figure 7. It can be seen that as φ approaches π, there is a substantial reduction in $G(t)$, although the difference tends to diminish at later times.

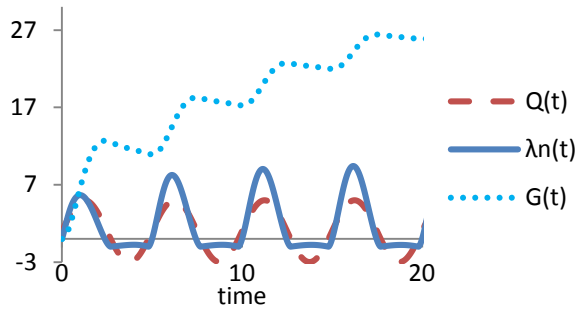

Figure 6 Profile of injection rate (Q), normalized growth rate ($\lambda_n(t)$) and integral of growth rate over time ($\boldsymbol{G(t)}$), at T=5, Γ=4, φ=0

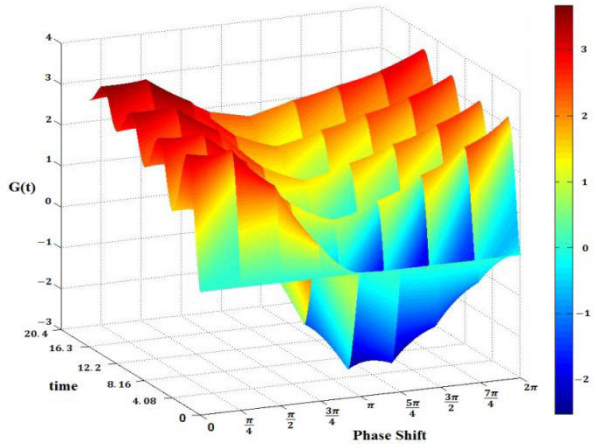

Figure 7 Profile of $\boldsymbol{G(t)}$ as a function of phase shift and time at T=5, Γ=1

Based on the previous results, it was attempted to modify the cyclic injection scheme by exploring similar schemes where the amplitude is now time-dependent. In particular, results for an amplitude that varies exponentially with time have been obtained, with different rates of decay. The adopted injection rate has the form:

$$Q = Q_C\left[1 + e^{Dt}\sin\left(\frac{2\pi t}{T} + \varphi\right)\right] \qquad (18)$$

This new model introduces an additional parameter that determines the rate of the temporal change of the amplitude. This approach attempts to reduce the growth of the amplitude to $\lambda_n(t)$, and therefore reduce $G(t)$ with time so as to make the displacement less unstable.

In order to ensure that the amount of fluid injected over a fixed period of time is the same when D≠0, the value of Q_C has been changed accordingly. Different values of the parameter D have been tested to determine its role in attenuating or enhancing the instability.

Figure 8 is a representative example of the results that illustrate how negative values of the parameter D can actually reduce the instability. It can be noted that as the parameter D decreases, the trends tend to smooth and stabilize almost asymptotically for Q and $\lambda_n(t)$.

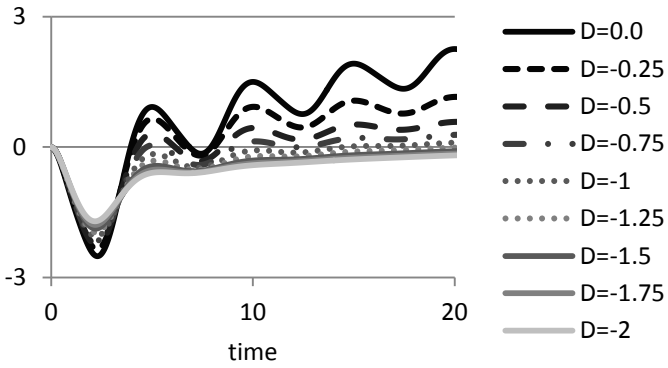

Figure 8 Variation of $\boldsymbol{G(t)}$ as D changes from 0 to -2, φ=π, T=5

It is clear that the application of time-dependent amplitude in the injection flow can considerably affect the development of instabilities in the linear regime. The use of this injection scheme might indicate that the application of sinusoidal injection schemes appears to play a bigger role in reducing instabilities at early times, but as the interface becomes larger, a constant injection scheme seems to be more adequate. Although a smaller interface may be more sensitive to the changes in the injection rate, the combination of shrinking amplitude and the impact of a small curvature may actually have stabilizing effects on the growth of the interface.

Monotonic Injection Schemes

In addition to the cyclic injection schemes, a number of monotonically growing flow injection schemes have also been analysed to explore their role in attenuating the instability. An exponential function was chosen to define the injection rate with respect to time. The parameters C and D are chosen by minimizing the function $G(t)$ through numerical integration and by fulfilling the constraint where:

$$\int_0^{t_c} Q_e(t)dt = Q_0 t_c \qquad (19)$$

With respect to linear injection schemes, two flow scenarios were investigated: one is based on the work of Dias et al. [16], where the parameters are defined as:

$$m = 2\pi(R_c - R_0)^2/t_c^2, b = 2\pi(R_c - R_0)R_0/t_c, \qquad (20)$$

and the other option is an extreme case where the injection starts at zero:

$$m = 2Q_0/t_c,\ b = 0. \qquad (21)$$

Trends for the variations of the relative growth rate (dashed lines) and the integral of growth rate (solid lines) for the linear and exponential injection schemes are shown in Figure 9. Based on these results, it can be concluded that the best way to ultimately minimize instabilities is to adopt a monotonic injection scheme, namely the injection profile proposed by Dias et al. [16].

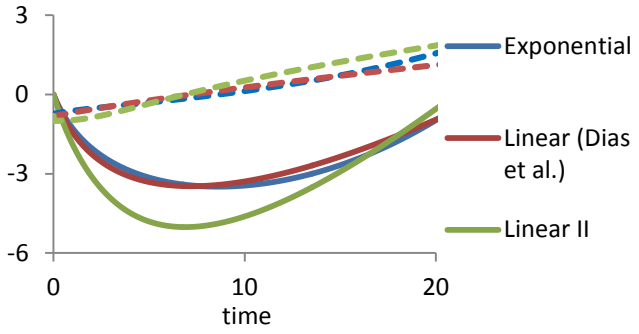

Figure 9 Relative growth rate $\lambda_n(t)$ (dashed lines) and the integral of growth rate over time G(t) (solid lines) for exponential and linear injection schemes.

CONCLUSION

Linear stability analysis indicates that most cases of cyclical injection schemes appear to lead to an increase in interfacial instability compared to the constant injection scenarios. However, a proper choice of the phase shift can actually reduce it at earlier times. Smaller period of the cyclic schemes tend to diminish the extent of instabilities with time; whereas larger amplitudes have a tendency to enhance the instabilities. A proposed scheme where the amplitude varies exponentially with time was found to substantially reduce the extent at which instabilities grow, showing that cyclic injection scheme might play a bigger role in reducing instability at the beginning of the injection process.

With regards to the monotonic injection schemes, the three models appear to lead to similar trends with respect to the growth rate of instabilities. Overall, this study reveals that among the different injection schemes, the two that have the potential to attenuate the flow instability are either the monotonic or the decaying sinusoidal injection schemes.

Acknowledgements

The authors acknowledge financial support from the Natural Sciences and Engineering Research Council of Canada (NSERC) and the computational resources from WestGrid.

REFERENCES

[1] C. T. Tan and G. M. Homsy, "Simulation of nonlinear viscous fingering in miscible displacement: Rectilinear flow," *Physics of Fluids,* vol. 29, pp. 3549-3556, 1986.

[2] K. Ghesmat and J. Azaiez, "Viscous fingering instability in porous media: Effect of anisotropic velocity dependent dispersion tensor," *Transport in Porous Media,* vol. 73, no. 3, pp. 297-318, 2009.

[3] S. D. R. Wilson, "The Taylor-Saffman problem for a non-Newtonian liquid," *Journal of Fluid Mechanics,* vol. 220, pp. 413-425, 1990.

[4] M. N. Islam and J. Azaiez, "Miscible thermo-viscous fingering instability in porous media. Part 1: Linear Stability Analysis," *Transport in Porous Media,* vol. 84, pp. 821-844, 2010.

[5] S. H. Hejazi and J. Azaiez, "Hydrodynamic instability in the transport of miscible reactive slices through porous media," *Physical Review E,* vol. 81, p. 056321, 2010.

[6] G. M. Homsy, "Viscous fingering in porous media," *Annual Review of Fluid Mechanics,* vol. 19, pp. 271-311, 1987.

[7] K. V. McCloud and J. V. Maher, "Experimental perturbations to Saffman-Taylor flow," *Physics Reports,* vol. 260, pp. 139-185, 1995.

[8] L Paterson, "Radial fingering in a Hele-Shaw cell," *Journal of Fluid Mechanics,* vol. 113, pp. 513-529, 1981.

[9] J.-D. Chen, "Radial viscous fingering patterns in Hele-Shaw cells," *Experiments in Fluids,* vol. 5, pp. 363-371, 1987.

[10] J.-D. Chen, "Growth of radial viscous fingers in a Hele-Shaw cell," *Journal of Fluid Mechanics,* vol. 201, pp. 223-242, 1989.

[11] O. Praud and H. L. Swinney , "Fractal dimension and unscreened angles measured for radial viscous fingering," *Physical Review E,* vol. 72, p. 011406, 2005.

[12] S. D. R. Wilson, "A note on the measurement of dynamic contact angles," *Journal of Colloid and Interface Science,* vol. 51, no. 3, p. 532–534, 1975.

[13] C-W. Park and G. M. Homsy, "Two-phase displacement in Hele-Shaw cells: experiments on viscous driven instabilities," *Journal of Fluid Mechanics,* vol. 141, pp. 257-287, 1984.

[14] L. M. Martyushev and A. I. Birzina, "Metastability at the displacement of a fluid in a Hele-Shaw cell," *Jounal of Experimental and Theoretical Physics letters,* vol. 99, no. 8, pp. 446-451, 2014.

[15] J. A. Miranda and M. Widom, "Radial fingering in a Hele-Shaw cell: a weakly nonlinear analysis," *Physica,* vol. 120, pp. 315-328, 1998.

[16] E. O. Dias, E. Alvarez-Lacalle, M. S. Carvalho and J. A. Miranda, "Minimization of viscous fluid fingering: A variational scheme for optimal flow rates," *Physical Review Letters,* vol. 109, p. 144502, 2012.

[17] E. O. Dias and J. A. Miranda, "Minimization of instabilities in growing interfaces: A variational approach," *Physical Review E.,* vol. 88, p. 062404, 2013.

[18] Y-S. Huang and C-Y. Chen, "A numerical study on radial Hele-Shaw flow: influence of fluid miscibility and injection scheme," *Computational Mechanics,* vol. 55, no. 2, pp. 407-420, 2015.

[19] Q. Yuan and J. Azaiez , "Cyclic time-dependent reactive flow displacements in porous media," *Chemical Engineering Science,* vol. 109, pp. 136-146, 2014.

[20] P. Daripa, "Studies on stability in three-layer Hele-Shaw flows," *Physics of Fluids D,* vol. 20, p. 112101, 2008.

[21] X. D. and P. Daripa, "Selection principle of optimal profiles for immiscible multi-luid Hele-Shaw flows and stabilization," *Transport in Porous Media,* vol. 96, pp. 353-367, 2013.